Supplemental Figure S1

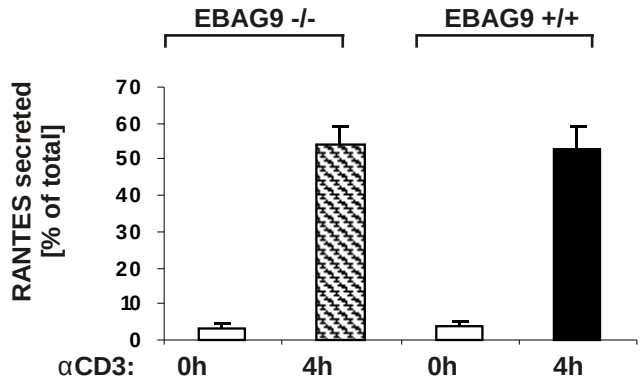

Figure S1. RANTES release from CTLs is unaltered in EBAG9$^{-/-}$ mice

CTLs were derived by MLR. Release of RANTES was triggered by TCR ligation with anti-CD3 mAb for 4 h and analyzed by ELISA (R&D Systems). Bars shown means ± S.D. of three independent experiments performed in triplicates.

Supplemental Figure S2

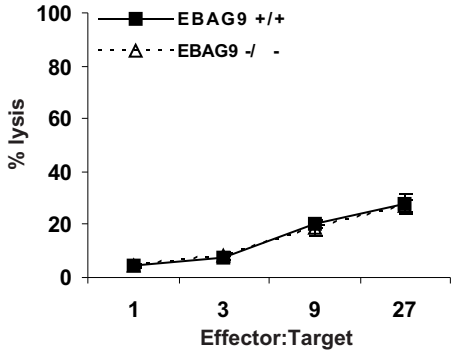

Figure S2. Enhanced allogeneic cytotoxicity of EBAG9$^{-/-}$ CTLs relies on the granule-mediated killing pathway
CTLs obtained from MLR were pretreated for 2h with 0.5 µM Concanamycin A (CMA; Alexis Biochemicals) and 5 µM Granzyme B inhibitor Z-AAD-CMK (Alexis Biochemicals) to block perforin/granzyme-mediated killing. Subsequently cytolytic activity of CTLs in the presence of CMA and Z-AAD-CMK against allogeneic P815 target cells was determined using Cytotox 96 nonradioactive kit (Promega) according to the manufacturer´s instructions and as described in *Methods*, respectively. Data are means ± S.D. of quadruplicates. One representative example of two experiments is shown.

Supplemental Figure S3

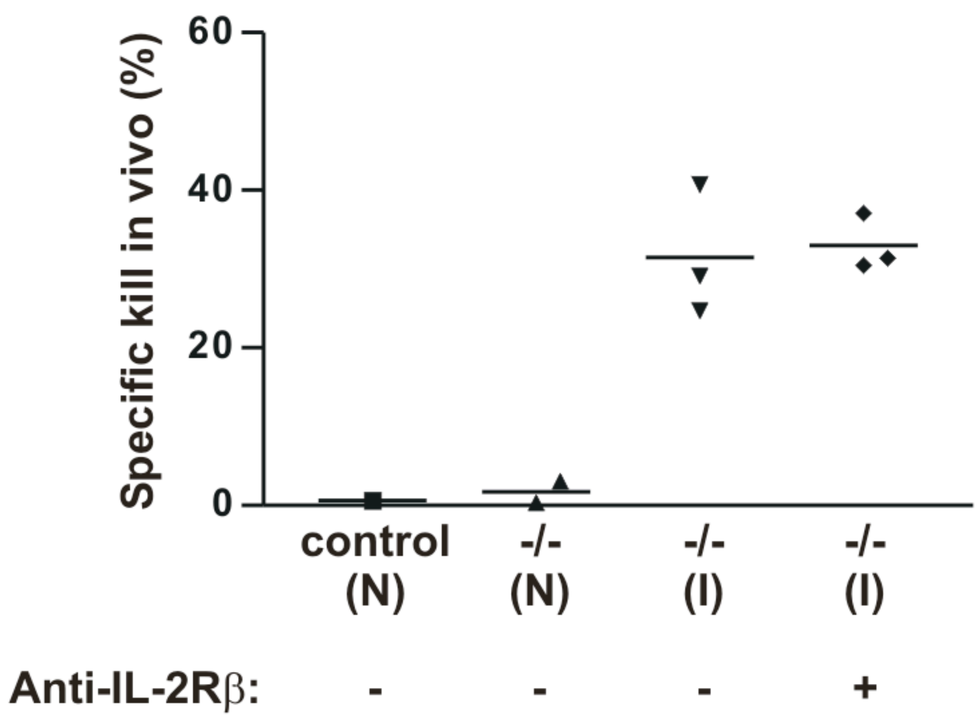

Figure S3. The rejection of Tag-loaded target cells is NK cell-independent

EBAG9$^{-/-}$ mice were immunized by injection (i.p.) of 2 x 10^6 Tag-expressing Co16.113 tumor cells. After 7 d, non-loaded and peptide-loaded spleen cells (1 x 10^7) from naive C57Bl/6 (B6) mice were labeled with different amounts of CFSE and injected (i.v.) into the indicated mice. After 4 h, the ratio between both populations in spleen of recipient mice was determined by flow cytometry. The percentage of specific killing of peptide-loaded cells is indicated, horizontal bars indicate mean values. Where indicated, NK cells were depleted by injection (i.p.) of 300 µg anti-IL-2Rβ mAb TM-β 1 on day three and 200 µg on day one prior to performing the killing assay. Depletion of NK cells was confirmed by FACS analysis (data not shown). In average, in untreated mice 4-5% NK cells were found in splenic splenocytes. Antibody-mediated depletion elicited a rate of < 0.4% NK cells. Control (N), naive wt mice; -/- (N), naive EBAG9$^{-/-}$ mice; -/- (I), immunized EBAG9$^{-/-}$ mice.

Supplemental Figure S4

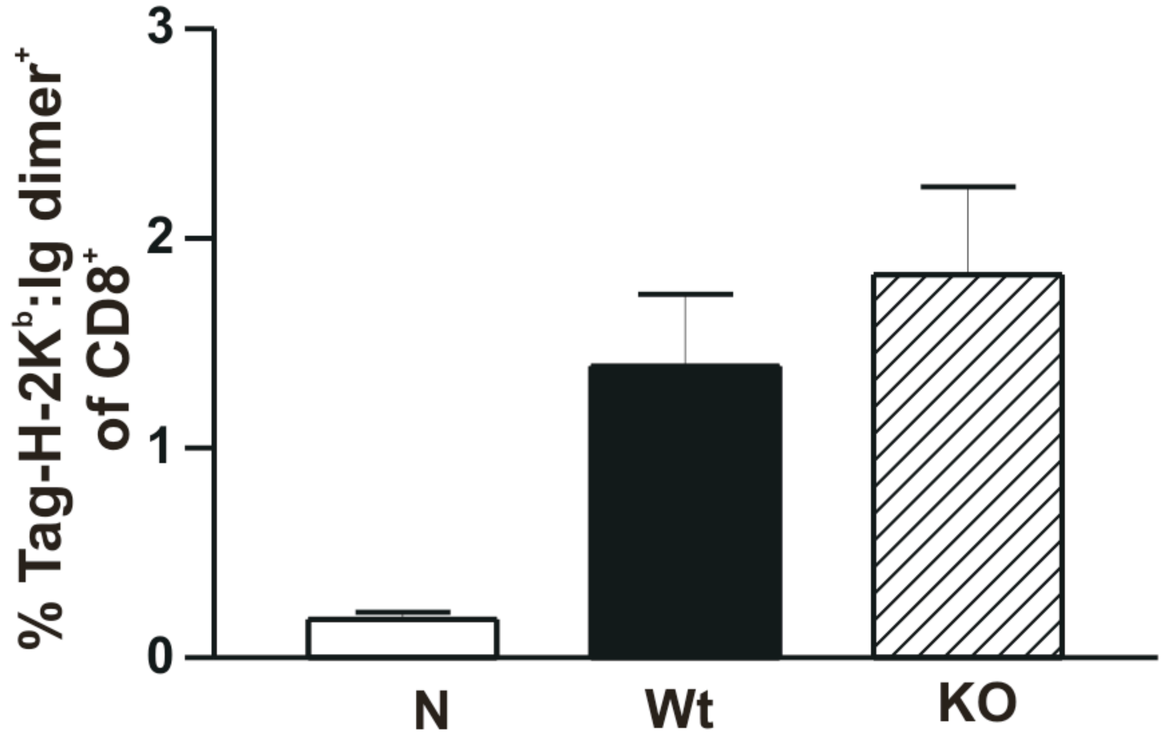

Figure S4. Frequency of antigen-specific CD8+ T cells during secondary immune responses

Mice were immunized as described in Figure 3A, followed by a boost after 30 d. At d 6 after rechallenge, splenocytes were stained sequentially with anti-CD8a mAb and H-2K^b:Ig dimers loaded with Tag-peptide, followed by flow cytometry analysis. N, naive Wt B6 mice. Bars, means ± SD of two independent experiments (n=5 for each genotype; no statistically significant difference).

Supplemental Figure S5

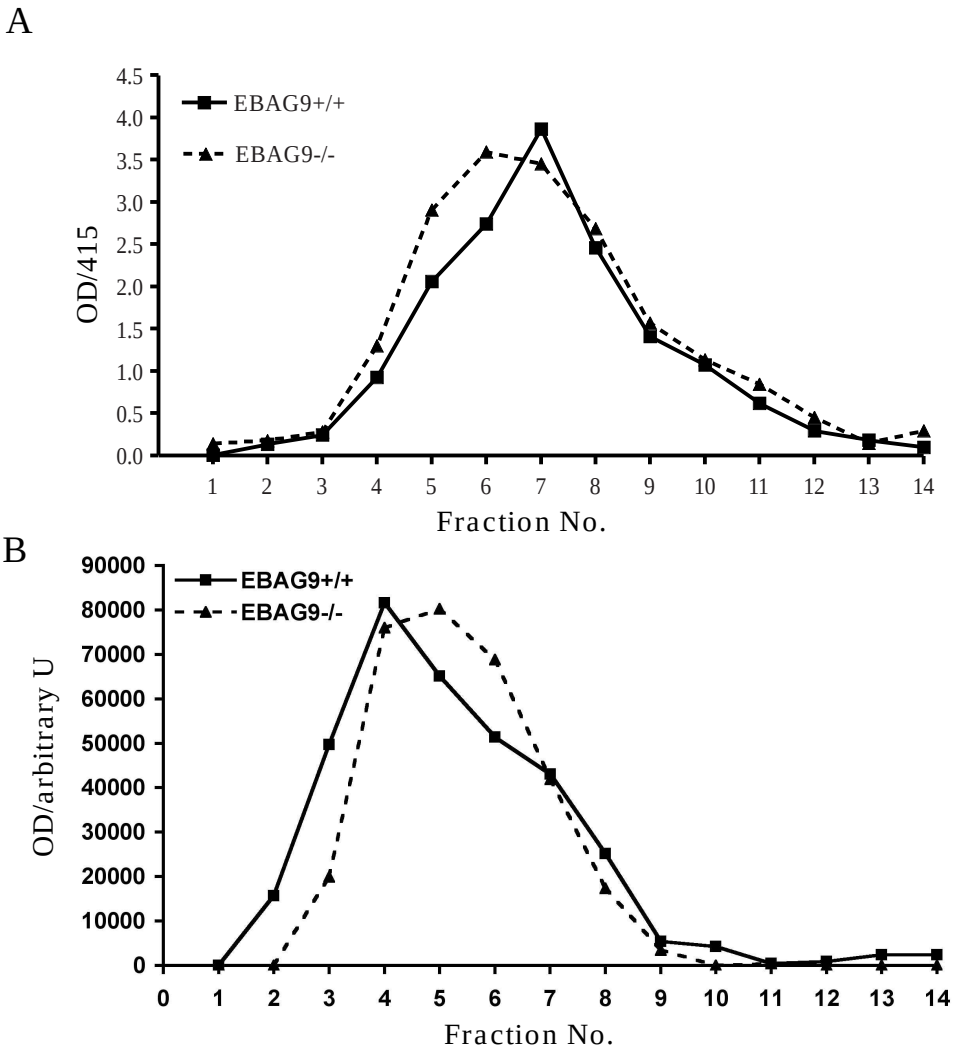

Figure S5. Re-distribution of the conventional lysosome marker ß-hexosaminidase

A postnuclear supernatant from 6 x 10^7 Wt and EBAG9$^{-/-}$ CTL (d6; n=3 mice per genotype) was centrifuged for 50 min to obtain a microsomal pellet. Microsomes were applied on a continuous OptiPrep gradient and subjected to centrifugation as described in Figure 10B. (A) Fractions were taken from the top of each gradient, followed by determination of ß-hexosaminidase activity in each gradient fraction using the substrate p-nitrophenyl N-acetyl-ß-D-glucosaminide (Calbiochem) in 100 mM citrate buffer/0.2% TX-100, essentially as described (Stinchcombe, J.C., et al., 2001. J. Cell Biol. 152: 825-834). After addition of 0.1 M carbonate buffer, pH 9.6, absorbance at 415 nm was read.(B) Distribution of the Golgi marker GM130 was determined by immunoblotting, shown is a quantification by densitometric scanning.

Supplemental Figure 6

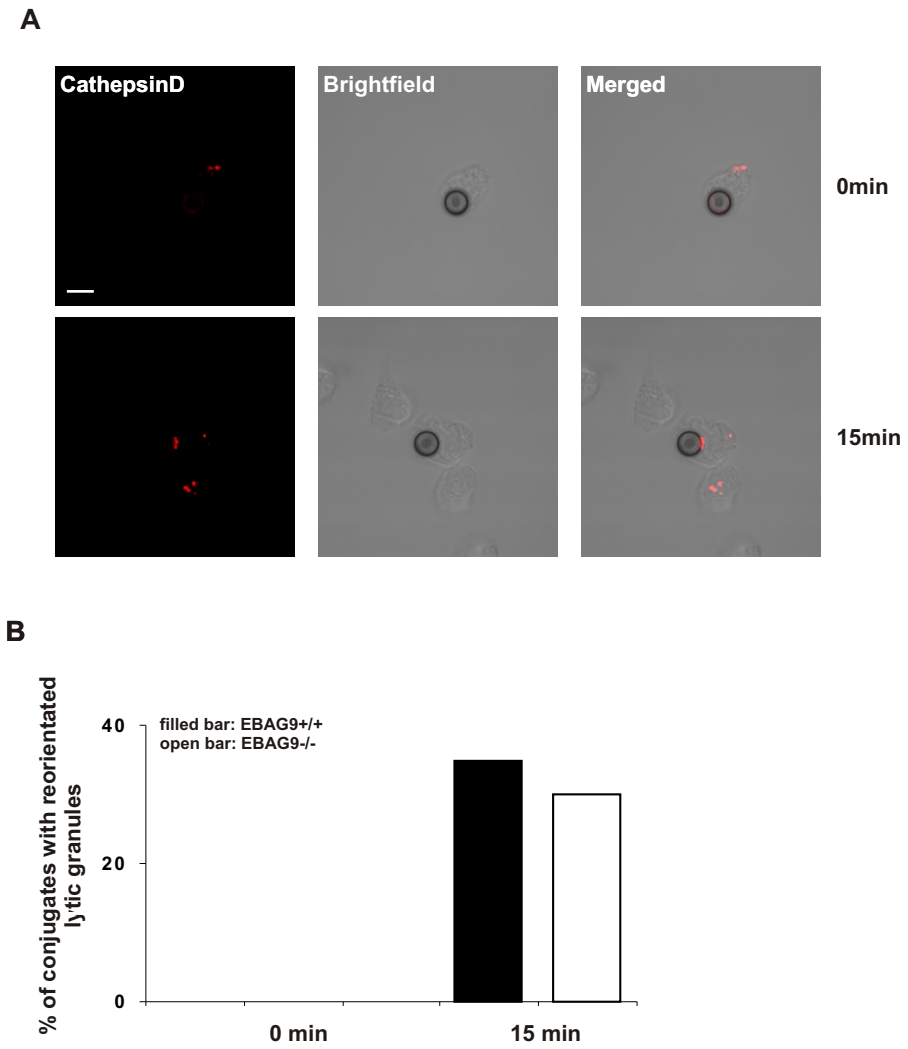

Figure S6. Secretory lysosome polarization toward the immunological synapse is indistinguishable between Wt and EBAG9$^{-/-}$ CTLs

CTLs were obtained from CD3/CD28 stimulation for 3 d, purified by negative selection with MACS beads, followed by *in vitro* culture for 2-3 d in the presence of IL-2 and IL-7 (50 U/ml). CTLs were mixed in a 1:1 ratio with CD3/CD28 precoated Dynabeads (4.5 m diametre), centrifuged for 5 min, and incubated for another 5 min at 37°C. Conjugates were plated on poly-L-lysine coated coverslips, and incubated for additional 15 min before fixation in acetone and permeabilization. Granules were visualized by intracellular staining with the secretory lysosome marker anti-Cathepsin D. Representative images of KO CTLs are shown. Polarization of Cathepsin D toward the contact site between T cell and microbead was seen exclusively after 15 min of incubation, but not at the 0 min time point. Unconjugated CTLs displayed discrete, punctate staining of intracellular Cathepsin D granules. The percentage of conjugates that displayed focused Cathepsin D is shown. Data are from one experiment with CTLs from n=3 animals per group, with at least 30 conjugates analyzed. Bar 5 m.

Supplemental Figure 7

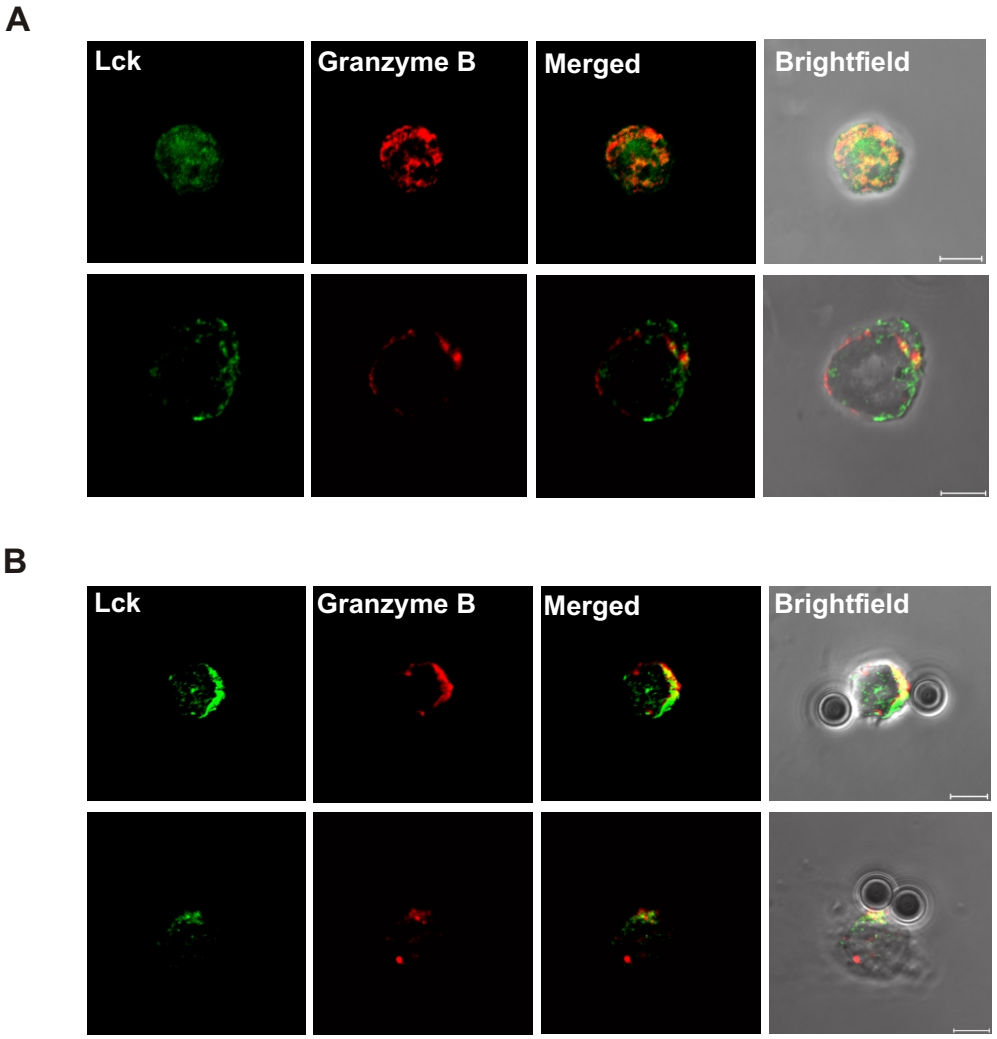

Figure S7. Immunological synapse formation is indistinguishable between Wt and EBAG9$^{-/-}$ CTLs CTLs from EBAG9 Wt and KO mice were generated and purified as in Figure S6. CTLs were mixed in a 1:1 ratio with CD3/CD28 precoated Dynabeads, centrifuged for 5 min, and incubated for another 5 min at 37°C. Conjugates were plated on poly-L-lysine coated coverslips, and incubated for additional 15 min before fixation with PFA and permeabilization. Granules were visualized by intracellular staining with the secretory lysosome marker Granzyme B-Alexa Fluor 647, and the signaling zone molecule Lck. Representative images are shown. At the 15 min time point, unconjugated T cells could be easily identified and exhibited a scattered, non-polarized distribution of lytic granules at the cell periphery (A). In T cells conjugated with microbeads, in both genotypes a clearly visible focusing of lytic granules toward the T cell-microbead interface occurred. In this polarized cluster of granules, substantial accumulation of Lck-positive structures was visible (B, Merged images). Data are representative of one experiment with CTLs from n=3 animals per genotype, with at least 20 conjugates analyzed. Polarization was identified in 6 synapses per group. Bar 5 m.

Supplemental Figure S8

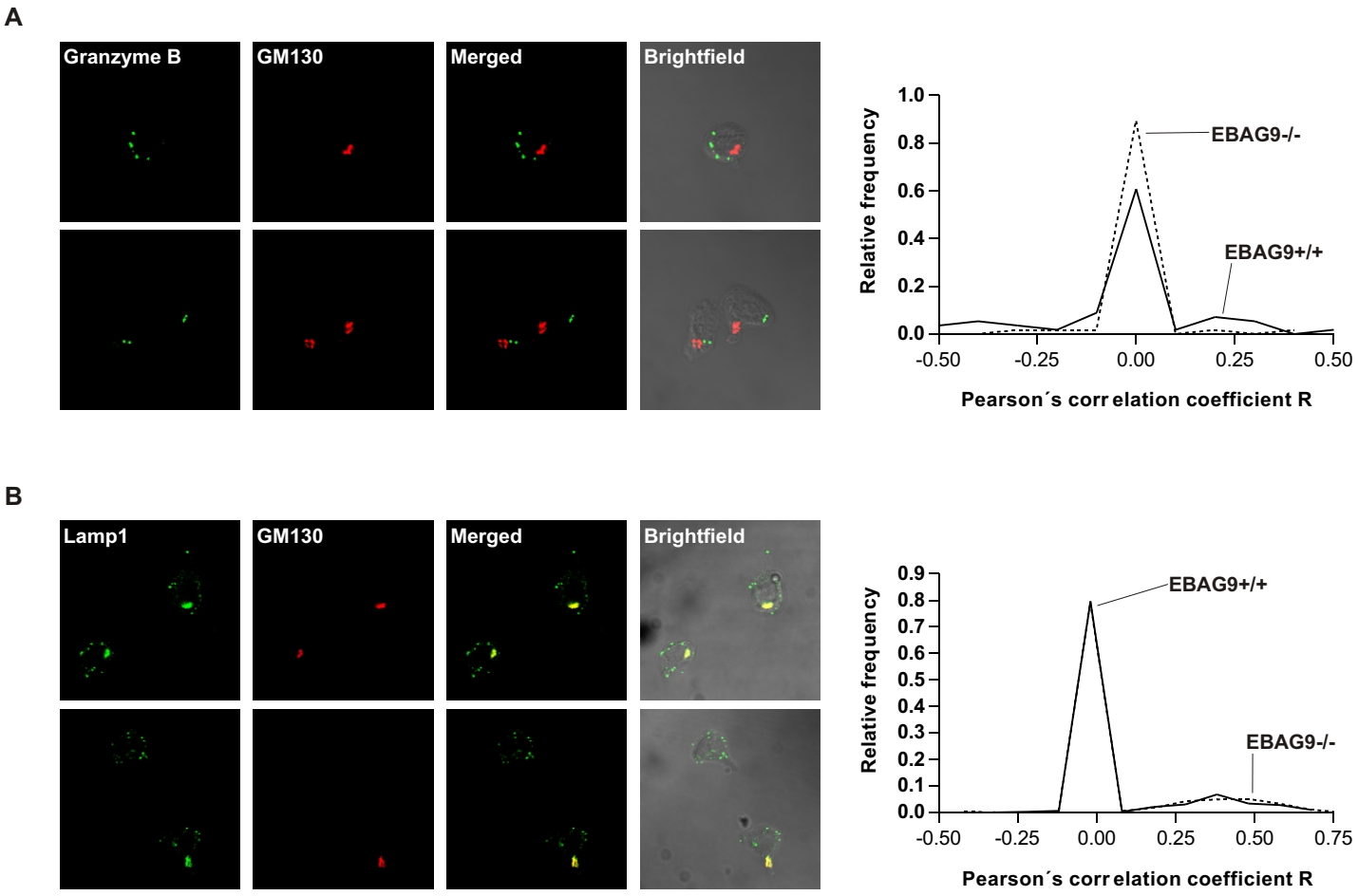

Figure 8. Subcellular localization of lysosomal compartment markers

(A) Colocalization of Granzyme B with the Golgi marker GM130. EBAG9$^{+/+}$, mean R = -0.026 (n = 56); EBAG9$^{-/-}$, mean R = -0.017 (n = 57); difference between EBAG9$^{+/+}$ and EBAG9$^{-/-}$ mice was not statistically different (p = 0.774, Student´s *t* test).

(B) Colocalization of Lamp1 with GM130. EBAG9$^{+/+}$, mean R = 0.074 (n = 325); EBAG9$^{-/-}$, mean R = 0.082 (n = 436); difference between EBAG9$^{+/+}$ and EBAG9$^{-/-}$ mice was not statistically different (p = 0.553, Student´s *t* test).

Supplemental Figure S9

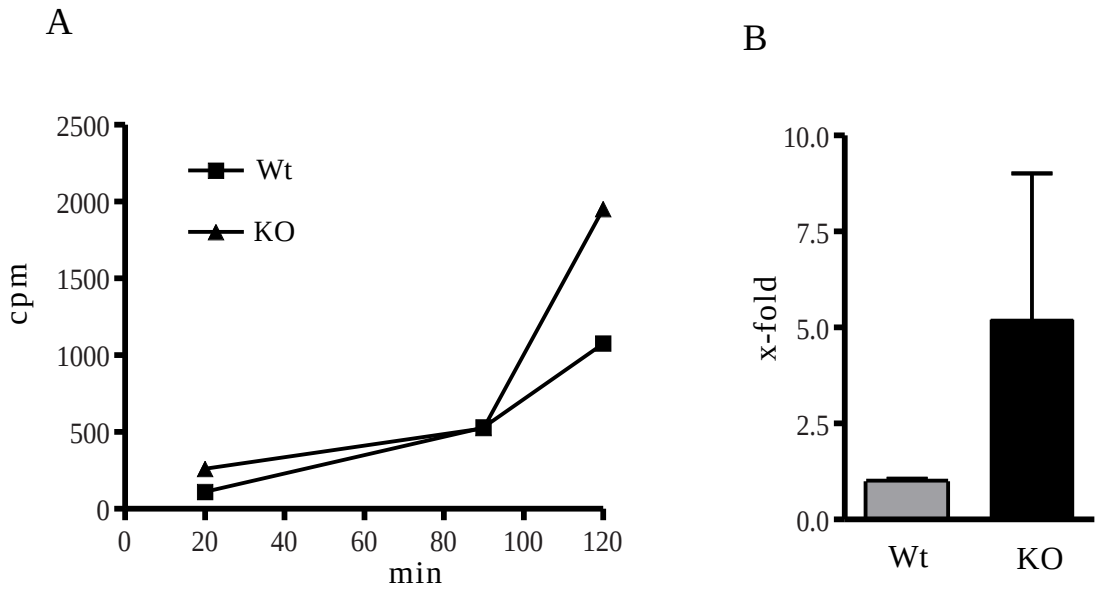

Figure S9. Intracellular transport of proteins is enhanced in CTLs from EBAG9-deficient mice

A) CTLs derived from Wt and EBAG9$^{-/-}$ mice were pulse-labeled with 500 µCi [^{35}S]methionine/cysteine for 5 min, and chased for 20, 90 and 120 min. For the chase period, equal numbers of cells (2 x 10^6/well) were transferred onto 6-well plates coated with CD3 and CD28 antibodies (inducible release), or onto untreated plates (constitutive release). At the time points indicated, cell-free supernatant was harvested, and TCA-precipitable radioactivity was determined. Total cell-associated radioactivity at the beginning of the chase period was comparable between genotypes. Regulated release for each time point (t) was calculated according to the formula:

regulated release= cpm (inducible release) - cpm (constitutive release). Data are representative of three experiments performed, with pooled CTL from a total of n=9 mice per genotype.

B) Values obtained according to this formula for the 2h time point from all three experiments were normalized for release in the Wt and set arbitrarily=1. Release is given relative to the rate in Wt cells, data represent mean values, and errors are shown as SEM; difference between Wt and KO CTLs was statistically significant.

Table S1. Hematopoietic parameters

Parameter	EBAG9+/+	EBAG9-/-
WBC (x 10^3/µl)	2.46 ± 0.54	2.78 ± 1.02
RBC (x 10^6/µl)	8.65 ± 0.35	8.80 ± 0.68
Hemoglobin (g/dl)	14.3 ± 0.5	14.8 ± 0.6
Hematocrit (%)	44.8 ± 2.1	44.8 ± 3.2
Platelet (x 10^3/µl)	965 ± 138	935 ± 101
% lymphocytes	82.1 ± 3.0	85.6 ± 2.5
% monocytes	5.74 ± 0.89	5.00 ± 0.72
% granulocytes	12.1 ± 2.3	9.42 ± 2.0
% $Ter119^+CD71^+$	17.6 ± 1.44	17.7 ± 1.3

Data shown are mean ± S.D. White blood cells (WBC), red blood cells (RBC), and other parameters in 8- to 12-week-old mice (EBAG9+/+, n = 14; EBAG9-/-, n = 15). Percent erythroid precursor (Ter119+CD71+) in bone marrow was determined by flow cytometry.

Table S2. Lymphocyte subpopulations in secondary lymphoid organs

Parameter	EBAG9+/+	EBAG9-/-	p value
Spleen			
% $B220^+$	49.6 ± 5.4	49.5 ± 4.6	n.s.
% $CD3^+$	35.4 ± 4	35.7 ± 4.3	n.s.
% $CD4^+$	20.3 ± 2.3	21.3 ± 2.1	n.s.
% $CD8^+$	14.3 ± 2	13.7 ± 1.3	n.s.
Lymph node			
% $B220^+$	37.4 ± 3.7	38.8 ± 7.3	n.s.
% $CD3^+$	60.3 ± 3.9	58.4 ± 7.4	n.s.
% $CD4^+$	36 ± 2.7	33.3 ± 6.6	n.s.
% $CD8^+$	23.4 ± 2.2	21 ± 3.4	n.s.

Data shown are mean ± S.D. (n=9) and were obtained by flow cytometry.